ANL/XFP/CP-102720

RECENT PROGRESS IN THE INVESTIGATION OF CORE HOLE-INDUCED PHOTON STIMULATED DESORPTION FROM ADSORBATES: EXCITATION SITE-DEPENDENT BOND BREAKING, AND CHARGE REARRANGEMENT.

P. Feulner, R. Romberg, S. Frigo (1) , R. Weimar, M. Gsell, A. Ogurtsov (2), and D. Menzel

Physikdepartment E 20, Technische Universität München, Germany

(1) Advanced Photon Source, Argonne IL, U.S.A.

(2) Verkin Institute for Low Temperature Physics & Engineering, Kharkov, Ukraine

Abstract

We report photon stimulated desorption (PSD) of neutral and ionic molecules and atoms from CO chemisorbed on Ru(001) and Cu(111), and from N_2 chemisorbed on Ru(001). Comparing branching ratios and spectral features for the O1s and N1s regions, we demonstrate that desorbing neutrals and ions are supplementary probes for the entire region of one- and multi-electron excitations, bearing valuable information on the transfer of energy and charge. For the primary [N1s]π^* excitation of N_2/Ru(001) we find excitation site-dependent branching into desorption of N_2^0, N^0 and N^+. PSD of neutral N atoms predominates for excitations of the N atom close to the surface, whereas mainly neutral N_2 molecules and N^+ ions are ejected for excitations of the outer N atom. We analyze the mechanisms of selective bond breaking on the basis of previously obtained atom-selective decay electron spectra. At the Ru3p substrate thresholds we find significant enhancements of the N^+ and N^{2+} yields from N_2/Ru(001), and discuss the electronic nature of the underlying energy transfer mechanism.

DISCLAIMER

This report was prepared as an account of work sponsored by an agency of the United States Government. Neither the United States Government nor any agency thereof, nor any of their employees, make any warranty, express or implied, or assumes any legal liability or responsibility for the accuracy, completeness, or usefulness of any information, apparatus, product, or process disclosed, or represents that its use would not infringe privately owned rights. Reference herein to any specific commercial product, process, or service by trade name, trademark, manufacturer, or otherwise does not necessarily constitute or imply its endorsement, recommendation, or favoring by the United States Government or any agency thereof. The views and opinions of authors expressed herein do not necessarily state or reflect those of the United States Government or any agency thereof.

DISCLAIMER

Portions of this document may be illegible in electronic Image products. Images are produced from the best available original document

Introduction

Bond breaking by selective excitations of core electrons is an interesting field of DIET for several reasons:

1. Core orbitals are well localized, at least in heteronuclear molecules, allowing allocation of the primary excitations to distinct atoms of the substrate-adsorbate complex. With narrow-band light sources even particular vibronic states can be selectively excited.
2. Core excitations very effectively drive dissociation and desorption. In most cases the decaying core holes give rise to doubly or even multiply (by cascades) excited valence states which are well localized and, if holes in bonding valence states are encountered, strongly antibonding. This antibonding nature of the excited states may even be enhanced for adsorbed species by charge transfer of screening electrons from the substrate into empty antibonding orbitals of the adsorbate /1/.
3. Upon decay, Auger or autoionization electrons are emitted as clear signatures of the decay route. They are useful pointers at subsequent electronically excited valence states. Correlating reaction products and decay electrons in coincidence experiments has developed into a commonly used tool for the investigation of core-induced photodissociation for isolated molecules. On surfaces, the strong background signal is a severe obstacle, and such experiments are much more difficult than in the gas phase. Nevertheless, impressive progress has been made, particularly for insulators, where DIET of ions prevails (see below) /2/. Present coincidence techniques for the surface /3/ are still limited in resolution by intensity reasons, for the electron energy as well as for the excitation bandwidth. Improved experimental performance with narrow-band excitation giving access to interference effects /4/ will be a promising field in the future.

RECEIVED
OCT 0 6 2000
OSTI

4. The sequence of core-excited and valence-excited states and the limited and well known lifetimes of the core holes give access to interesting details of the reaction dynamics, in particular if strongly antibonding core-excited states are selected as, e.g., the energetically lowest excitations of the halogen, or chalcogene hydrides, and multi-electron excitations of other molecules. Electron spectroscopy and calculations provide clear evidence that bond breaking can occur *before* core decay, identifying the core-excited state as an important source of kinetic energy /4-9/.
5. Finally, the possibility to allocate the excitations to distinct atoms enables the study of resonant energy transfer processes. The interatomic Auger decay of the Knotek-Feibelman mechanism is a well known example /10/. Longer range interactions as observed in photoemission and explained as Multi Atom Resonant Photoemission (MARPE) /11/ can be expected in DIET as well.

To experimentally study these topics in detail, analytical tools are required in particular for the reaction products. For isolated molecules and DIET from insulator surfaces, neutralisation by substrate-adsorbate charge transfer is missing or weak, and ionic reaction products prevail /1/. For DIET from chemisorbed or physisorbed layers on metals the situation is completely different. In most cases, ions predominate only for exotic primary multi-electron states with very low excitations cross sections. For one-hole and even for many two-hole states the DIET products, molecules or fragments, are emitted as neutrals (see below). As these excitation channels clearly constitute the majority and are most important for any kind of technical application, means for the detection of neutral particles are urgently needed. State selective optical methods (REMPI or LIF /12/), and state integrating methods based on mass

spectrometers compete, the latter utilizing post-ionization either by electron impact or non-resonant multi photon ionization. In combination with monochromatized synchrotron radiation, all laser-based optical methods suffer from the misfit of the repetition rates of the storage rings on the one hand (typically more than one MHz), and of the lasers on the other (less than 1 kHz), which wastes useful signal. Moreover, particularly molecules commonly desorb in many quantum states /13/ which makes yield measurements with resonant techniques very time consuming. We have neglected therefore in a first approach the distributions of internal energies, and have chosen a mass spectrometer device with electron impact ionization for the detection of neutral particles. The most severe disadvantage of this method is the strong coupling of fragment and parent signals by cracking inside the ionizer. It can be mastered by careful calibration of the instrument with well-known sources, and by operating the ionizer with different electron fluxes and electron energies which strongly affect the cracking behavior. First results for CO/Ru(001) have been reported at DIET-7 /14/. Since then, considerable progress has been made in sensitivity which now allows us to detect even "difficult" particles such as neutral hydrogen atoms /15/, and makes measurements under high resolution conditions possible (see below). By pulsed operation of the ionizer and recording of the TOF distribution behind the mass filter, kinetic energies of fragments and molecules are now measurable and can be compared with kinetic energies of the respective ions /16/. Electron and ion TOF techniques are also used for the determination of ionization edges /17/, and for investigations of kinetic energy distributions of emitted ions /16/. Because of the limited space available here, all experimental details are presented in other contributions to this conference /15,16/. Instead, a survey is given in the next chapter on the importance of DIET of neutrals by core excitation comparing ion and neutral yields obtained from CO

chemisorbed on Ru(001) and Cu(111), and from N_2 on Ru(001). We then inspect DIET by π-resonant excitation of N_2/Ru(001) more closely, particularly concentrating on the importance of the intramolecular excitation site. Finally we focus on fragment desorption by core hole excitations of the substrate and discuss possible scenarios of the energy transfer.

DIET by core-excitations from chemisorbates: A comparison of ion and neutral yields. In Figs.1 - 4, the partial electron yields (PY), and the ion and neutral particle yields from a) CO/Ru(001), b) CO/Cu(111) and c) N_2/Ru(001) stimulated by O1s and N1s excitations are displayed. To ease comparison, all excitation energies are referred to the energy position of the π-resonance. For all systems the molecules are adsorbed in upright positions in well ordered layers. We only show spectra for A_{xy}-light with the **E**-vector perpendicular to the molecular axis, because more resonant structures appear for this polarization than for A_z (a more complete discussion of these measurements will be given in forthcoming papers /18,19/). Systems a) and c) were prepared directly on the (001) plane of the Ru substrate, and b) on a (111) oriented Cu layer epitaxially grown on the Ru substrate. ($\sqrt{3}$x$\sqrt{3}$)-layers were prepared by dosing CO or N_2 in excess, and controlled thermal desorption and annealing. We have selected these systems because they span a wide range of substrate-adsorbate bond strength, although their electronic states are very similar. CO and N_2 are isoelectronic molecules, mainly characterized by their different symmetry, and the electronic nature of the surface adsorbate bond varies only gradually /20,30/. CO/Ru(001) is rather strongly bound and desorption is completed only around 640K /21/, whereas N_2 is weakly bound (complete desorption by 120 K), requiring sample temperatures below 85K for irreversible adsorption

/22/. The chemisorptive bond of CO/Cu is stronger than for N_2/Ru, but much weaker than for CO/Ru.

The data reveal a rather clear trend. We first focus on CO for which stimulated desorption of ions is well known from previous experiments /23/. For both Ru and Cu, photoabsorption monitored by the partial electron yield is dominated by the [O1s]2π-resonance (Fig.1). The [O1s]6σ shape resonance is invisible for A_{xy}-light. At its position we find a small peak that in previous PSD experiments has been assigned to a 2h2e state with mainly [O1s1π]$2\pi^2$ contribution /23/. This assignment has been corroborated by calculations /24/ as well as by polarization resolved photoabsorption measurements in the gas phase /25/. An additional resonance appears in the ion signals, particularly for the fragments O^+ and C^+, at 36 eV above the π-resonance. It has been assigned to a 3h3e state with π-symmetry, probably [O1s$1\pi^2$]$2\pi^3$ /23/. In the PY signal this structure is absent because of its small excitation cross section. At this resonance the yield of fragment ions increases dramatically for Ru and Cu (Fig.1). In the CO^+ signal it is weakly visible. By comparing CO^+ and O^+ yields on an absolute scale, we find that molecular ions are always an extremely rare species. At the π-resonance (i.e. at the energetic position where the excitation cross section is largest by far) the two signals are of similar size, whereas O^+ exceeds that value by far at higher resonances where the primary excitation cross sections are certainly lower by orders of magnitude.

Comparing now the relative shapes particularly of the fragment signals for Ru and Cu, we find the multi-electron excitations less strongly pronounced for the more weakly bound CO/Cu. Obviously, less repulsive primary and secondary states (after core-hole decay) and less

positive charge on the CO is needed for ionic desorption from Cu. This is best seen for DIET of C^+, which for Cu occurs even for π-resonant excitation, whereas for Ru the signal is negligible below the 3h3e state /23/. The less perfect screening on Cu due to the lower electron density at the Fermi edge enables DIET of C fragments as ions, which for Ru only desorb as neutrals, the spectral yield features of which we discuss next (Fig.2).

From CO/Ru and CO/Cu, we find PSD of CO^0, O^0 and C^0 (not shown). At the π-resonance the CO^0 signal is larger than the O^0 signal by a factor of 3.5 for Ru, and 2.8 for Cu. The spectral shapes of the signals resemble that of the PY, the π-resonance being the largest feature, although the 2h2e state is more pronounced compared to the PY /14/. Its relative enhancement is small for the CO^0 signals and larger for the O^0 fragments. Comparing Ru and Cu, we find a similar trend as for the ions. The enhancement is smaller for Cu than for Ru. This is due to the stronger bond and the stronger coupling for the transition metal Ru which more efficiently quenches bond breaking compared to the noble metal Cu. For Ru as well as for Cu, the 3h3e state does not appear in DIET of neutrals.

We emphasize that by measuring neutrals we do not monitor "minority" channels, neither in primary excitations nor in reaction products, as we do in the case of ion PSD. First of all, the sensitivity of our equipment is by far not sufficient to compete with the detection of ions. Secondly, we find examples like DIET from CO/Cu where the spectral shape of the yield is very close to the primary excitation rate and more repulsive states are not significantly enhanced, which clearly means that the escape probability of neutrals even for 1h1e excitations cannot deviate by orders of magnitudes from one as it does for ions. We further

know that we monitor true PSD and not X-ray induced electron stimulated desorption (XESD) because the kinetic energy distributions at least of the O-atoms are different for the region below the O1s edge, for the π-resonance, and for the 2h2e state /16/.

Weakly chemisorbed N_2/Ru(001) is our next example, and we analyse PSD of N^0 and N_2^0 first (Fig.3). As for CO, we find PSD and PY closely related, however not in every detail. The π-resonance is the largest feature and structures beyond 20 eV which predominate the ion signals (see below) are absent. Above the π-resonance two maxima appear in the N^0 yield (and less strongly pronounced in the N_2^0 signal) at 10 and 15 eV, which clearly can be assigned to 2h2e-valence excitations. Calculations of Arneberg et al. for the isolated N_2^0 molecule have predicted a variety of 2h2e states around and slightly above the $N1s^{-1}$ threshold, from 9.5 to 11.9 eV above the π-resonance, at 14 eV, around 17 eV and from 19 to 23 eV /26/. The 14 eV structure has clearly been resolved in polarization integrated /27/ as well as polarization resolved photoabsorption /28/. It has π-symmetry /28/ and exhibits two vibrational progressions separated by about 1 eV with small, but different vibrational quanta /27/. The contribution with the lower energy has tentatively been assigned to the $[N1s3\sigma_u]1\pi_g3s\sigma$ state, and that at higher energy to the $[N1s1\pi_u]1\pi_g3p\pi$ transition /27/, in agreement with Arneberg's calculations ($[N1s1\pi_u]1\pi_g2\pi_u$ /26/). PSD is expected to project out the most dissociative component. The small, but clearly resolved blue-shift of this peak in the N^0-PSD signals with respect to the PY (and the N_2^0 signal !) could at least partly be due to the higher fragmentation yield obtained for the $[N1s1\pi_u]1\pi_g3p\pi$ component of the excitation (see however below).

The electronic nature of the maximum at 10 eV has been revealed only recently. Studying anisotropy parameters, Lee et al. found that the assignments made by Chen et al. on the basis of the equivalent core approximation were at least partially incorrect because of an excess of π-state density in this region, and they reassigned some of these transitions, however not questioning the Rydberg character of these states /29/. By carefully analyzing decay electron spectra Neeb et al. demonstrated that from excitations in this range some percent of the total decay intensity appear in atomic lines, and concluded that the additional π-intensity is not due to Rydberg transitions, but to dissociative 2h2e states as already predicted by Arneberg's calculations /8,26/. Our PSD data are in perfect agreement with these results. The main contribution is the $[N1s1\pi_u]1\pi_g^2$ configuration, i.e. that one which for CO is seen at 15 eV. We emphasize that we certainly do not see only the few percent of decay events that in decay spectroscopy had been identified as ultrafast. The maximum at 15 eV which belongs to a non-dissociative primary state because it exhibits vibrational structure in the gas phase /27/ appears with comparable intensity. Valence excited post-decay states which, due to their double holes, may be repulsive and are well localized, will contribute most, but a strongly repulsive primary excited state will certainly contribute kinetic energy, although only a small fraction of the core holes will survive dissociation. We find that the energy positions of these multi-electron excitations with valence character are not strongly shifted with respect to the π-resonance upon chemisorption, because very similar ΔE values are obtained for the isolated molecule, and for weakly as well as more strongly chemisorbed particles. We further note that the valence character of these excitations around $\Delta E = 10$ eV is clearly revealed from their persistence in the photoabsorption signal upon chemisorption, which red-shifts the N1s threshold by a few eV, and would quench any states with true Rydberg character in this energy

range. (The $[N1s1\pi_u]1\pi_g3p\pi$ state is certainly not a real Rydberg state because of its double hole charge.)

In this context particularly the N^0-spectrum reveals some surprising details. We will show below that PSD of neutral N atoms dominates for excitations of the inner N atom that is close to the surface. Two interesting details of this spectrum are the well-resolved step at the Fermi edge to the left of the leading edge of the π-resonance, which is in perfect agreement with data on decay spectroscopy /30/, and the rather large desorption signal between the π-resonance and the onset of the multi-electron states around 10 eV. In the N_2^0 signal (which mainly is emitted for excitations of the outer N atom, see below) the intensity is zero in this energy range. This is surprising, because threshold electron spectroscopy with the method of ref.17 yields vanishing intensity of one-hole states for the inner N atom from the threshold up to several eV above. The comparatively large photoabsorption cross section deduced from PSD of N atoms in this energy range must mainly be due to excitations of satellite states. Because of lacking molecular electronic levels close to the π-resonance, these states must be metal derived, and strong transitions obviously exist only for the inner N atom in agreement with the selective appearance of the Fermi step. Because near threshold the photoelectron yield is very similar for the inner N atom of chemisorbed N_2 and the C atom of chemisorbed CO on the one hand, and for the outer N atom and the O atom on the other, we predict the existence of similar transitions for C1s excitations of adsorbed CO. Their interaction with 1h states possibly could explain the efficient vibrational relaxation that has been seen in XPS for C1s but not for O1s ionization /31/.

The N^+ and N^{2+} signals from N_2/Ru(001) behave dramatically different from the PY or the PSD of neutrals (Fig.4). Desorption of N_2^+ is extremely weak, and completely absent at the π-resonance. The π-resonance and the two 2h2e states are strongly depleted in N^+ and become visible only after considerable magnification of the data in this region (Fig.4). No N^{2+} emission occurs in this range. A strong increase of N^+ and N^{2+} PSD sets in around 20 eV with broad maxima around 26 and 38 eV, and steps at absolute photon energies of 460 and 481 eV. The latter two steps are due to excitations of the Ru 3p levels, the coupling of which to the adsorbed N_2 will be discussed in the last chapter. By comparing the N_2 and the CO data, we explain the strong increase around 20 eV as the onset of 3h-state formation, either of shake-up (maxima) or of shake-off nature (increasing background). No calculations exist as yet. Our assignment would mean that the threshold for 3h configurations is lower in N_2 than in CO. We believe this to be reasonable, because also 2h2e configurations appear at considerable lower energy as for CO and because mixing of configurations is more important for N_2 than CO.

Corroborating similar conclusions of previous studies, we stress again that PSD of ions due to its selectivity is a perfect spectroscopic tool for the investigation of very rare electronic excitations in adsorbed and condensed species. However, if majority channels are of interest, as in all technically oriented investigations of degradation and desorption by irradiation, neutrals are the favorite species to be monitored. This has been shown for valence excitations long ago by MGR /32/ and it is obviously also true for DIET by core electron excitation. To demonstrate the potential of our method, we focus on DIET from N_2/Ru(001) by π-resonant

excitations. Tiny deviations of the shape of the π-resonance are clearly visible for the different species in Fig.3. Switching to high energy resolution, we will study these differences next.

Excitation site-dependent bond breaking

Fig.5 displays PY, N^+-PSD, N^0-PSD and N_2^0-PSD traces obtained from N_2/Ru(001) around the π-resonance by excitation with a photon bandwidth of about 150 meV. The individual traces are obviously composed of two components in varying mixtures that are separated by 0.7 eV in energy. For N_2/Ni(100), similar bimodal photoabsorption distribution curves have been obtained and explained by different resonance energies for the outer (oriented towards the vacuum) and the inner (close to the substrate) N atoms, i.e., the degeneracy of the two $[N1s]\pi^*$ states is lifted by the symmetry breaking introduced by chemisorption /33/. Our PY curves corroborate data previously obtained for N_2/Ru(001) from decay electron spectroscopy /30/. Excitations of the different N atoms yield different decay spectra, and by their careful analysis the spectral shapes of the two components contributing to the π-resonance peak could be extracted for Ru /30/ as well as for Ni /33/. The contribution with the higher excitation energy belongs to the inner N-atoms /30,33/.(We note that even with better photon energy resolution vibrational fine structure remains absent for N_2/Ru, in agreement with results for Ni /33/, and as expected for chemisorbed species.)

Our measurements show that not only the photoabsorption exhibits bimodal behavior, but also the PSD signals, and that the contributions of excitations located at the outer/inner N atom are differently weighted for the different reaction products. Even a coarse analysis of the data shows that excitations of the outer N atom contribute mainly to the N_2^0 and N^+ signals (recall that the latter particles are an extreme minority species at the π-resonance, see above),

whereas N atoms desorb predominantly by excitations of the inner N atom. For a quantitative analysis, we use Keller's deconvolution of the PY signal into the contributions of the inner and outer excitations on the basis of atom-selective decay electron spectra /30/, which after an 5% adjustment of the relative amplitudes accounting for the different angular acceptances in the two experiments perfectly reproduces our PY data, see Fig.5, and fit our PSD curves by linear combinations of the two components. We obtain best fit results for main contributions of: 78 ± 2% *outer* component for N^+-PSD, 77±3% *outer* component for N_2^0-PSD, and 65±4 *inner* component for N^0-PSD (to account for the increasing N^0 signal due to transitions into metal derived states, a small background signal linearly increasing with photon energy has been added here). We arrive at these numbers by taking the experimentally obtained ratio of the two components. If we normalize their amplitudes, i.e. divide by their different excitation cross sections in order to obtain results on a "per photon" scale, the above numbers change to 84%, 83% and 56%, respectively. In summary, we find that photodesorption of atomic ions and neutral molecules is mainly due to excitations of the *outer* N-atom, whereas fragmentation is enhanced if the *inner* N-atom is π-resonantly excited.

We explain these excitation site-selective branching ratios on the basis of recent decay electron spectroscopy data /30/, and the electronic nature of the chemisorptive bond of N_2 that has been derived from X-ray emission data. In ref.20 it was shown by atom-selective experimental and theoretical results that the chemisorptive bond of nitrogen can be described by an allylic configuration comprising the two N as well as the nearest metal atom, resulting in a system of three π-orbitals. That with the largest electron binding energy is bonding with respect to all three atoms. It is mainly derived from the $1\pi_u$-MO of the isolated N_2, with small,

but significant contributions from metal d-states. The second π-orbital is essentially non-bonding with mainly metal character. The highest π-orbital is antibonding for the adsorbate and the intramolecular bond. It is derived from the π^*-MO of the molecule, with contributions from metal d and p states. For N_2/Ni(100) it was found to be unoccupied and is expected to be here as well; it plays a role as screening orbital upon core hole creation. The σ-orbitals are polarized in a way that minimizes repulsion with metal sp states /20/. Contributions of ultrafast bondbreaking to our PSD signals can be excluded, for the decay of the intramolecular as well as for the N_2-metal bond, because i) the π-resonance is a bound molecular state, and ii) the difference in potential energy for Ru-NN^* and for Ru-N^*N is of the order of the chemisorption energy of Ru-NO (the equivalent core analogue to Ru-NN^*) which is not more than 1.6 eV /34/. Considering the large mass of NO, possible potential gradients are too small to cause bond breaking during the N1s lifetime. The final states after the core decay, however, are very different for outer or inner N1s excitations. Inner N1s holes mainly decay into final states with $[1\pi^2]$ and $[1\pi 4\sigma]$ double holes (we use the $C_{\infty v}$ nomenclature of the molecular orbitals, stressing the lack of homonuclear symmetry), whereas $[5\sigma^2]$, $[4\sigma^2]$ and $[4\sigma 2\pi]$ hole configurations dominate for outer excitations /30/. We further note that we have to consider full relaxation of the final states after core decay for the time scale of PSD, i.e., 2h2e states, with the topmost π-orbital as screening orbital. The 1π-orbital is strongly bonding with respect to the molecular bond, and a double hole efficiently dissociates the nitrogen molecule, in particular if the additional charge transferred into the energetically highest, overall antibonding π-orbital is taken into account. This explains the large N atom signal for selective excitation of the inner N atom, whereas most decay states of outer excitations leave the intramolecular bond intact (we neglect the tiny N^+-signal, which clearly is a minority species

which cannot easily be traced back to the majority channels of the decay spectrum). The intramolecular bond is weakened less by 4σ and 5σ holes, which predominate the decay states of outer excitations, than by 1π-holes which prevails for inner excitations. For the substrate-adsorbate bond these σ-orbitals are mainly repulsive and their ionization should not weaken the bond at all. The strength of the metal-adsorbate bond is however decreased by the transfer of screening charge into the antibonding, topmost π-orbital, and probably also by an increase of the 1π-binding energy due to the positive charge in the σ-states. Such a blue-shift of the binding energy of the all-bonding π-orbital depletes its coupling with metal states and weakens the adsorbate bond. Although the occupation of the antibonding π^*-orbital by screening electrons is likely to be similar for double 1π-holes on the one hand and double σ-holes on the other, we find less fragmentation events because the intramolecular bond is weakened more for the 1π double hole than for the 4σ and 5σ double holes. (We note that our analysis is not complete because, e.g., all final states containing holes in inner valence levels (3σ) have not been not included because of lacking decay electron data. The existence of these minority channels explains why the decompositions of our PSD-spectra are not "pure", but only show strong enhancements according to the main decay channels that dominate for the individual PSD species).

Core hole excitation-induced energy transfer studied by DIET

We finally come back to PSD of ions which historically contributed most to our field of science. A very exciting detail is DIET by electronic excitations in the substrate. In the low energy range hot electrons proved to be a an effective stimulant for DIET /35/. For the high energy range Knotek and Feibelman proposed that energy could be transferred by interatomic

hole decay from the substrate to the adsorbate bond /10/. Although Feibelman's idea to make DIET a versatile tool for the investigation of surfaces did not come true (i.e, in particular to overcome the minority problem encountered in DIET of ions, see above), the model stimulated the field of DIET for many years. During the last year, a mechanism labeled MARPE (multiple atom resonant photemission /11/) attracted considerable interest in photoelectron spectroscopy. It describes the transfer of excitation from a host medium to embedded or adsorbed atoms. Whereas similar processes are well known for valence excitations /38/, they were new and rather unexpected for core-excited states /11/.

In Fig.4 it was shown that the N^+ and N^{2+}-PSD signals from N_2/Ru(001) increase at the $Ru3p_{3/2,1/2}$ substrate thresholds. In Fig.6 both signals are compared with the PY. The PY and the PSD data have been obtained simultaneously. The onsets of the ion signals are blue-shifted by about 1 eV with respect to the PY which monitors the photoabsorption. We believe that the existence of this shift clearly rules out that the ion signals are due to XESD. True XESD signals like N_2^+ from non-perpendicularly bound N_2/Ru(001) or CO^+ from CO/Cu(111) perfectly mimic the spectral shape of the PY. Moreover, Ru 3p holes mainly decay by Coster Kronig transitions into Ru 3d holes which limits the decay electron energies to about 270 eV. For electron energies below 420 eV, however, the N^+-ESD cross section is very small /37/. Ru3pVV transitions that would yield higher electron energies are extremely rare, and even those electrons would not strongly contribute to the N^+ yield, because the ESD cross section reaches its maximum not below 800 eV /37/. Because desorption cannot be due to ESD, the excitation must be transferred directly from the Ru surface atoms to the nitrogen molecule, and the observed blue-shift must be a result of this energy transfer. We stress that the

excitation of the N_2 molecule that is brought about by that energy transfer most probably is a *multi*-electron *core*-excited state, because *one*-electron core excited states yield vanishing N^+ and N^{2+} intensity, as do *multi*-electron valence states which would show up in the pre-threshold signal (see Fig.4). We believe that the enhancement of the ion signals is due to a direct coupling of the Ru3p threshold resonances, and the N1s multiple shake-off continuum that dominates the ion signal (see Fig.4). The mechanism is very similar to MARPE, apart from the fact that not photoelectrons but desorbing ions are detected.

The exact nature of the blue-shift remains unclear, however. A value of 1 eV is probably too large for a surface core level shift. Reported core level shifts for Ru 3d levels are in the range of 0.3 eV, apart from oxygen, which causes larger shifts /38/. Particularly the shift induced by molecular adsorption (CO) is small /38/. Larger shifts can only be expected if the chemisorptive energy on the Z+1 substrate is very different, which for molecular chemisorption only occurs for those transition metals that neighbor noble metals like Pd /39/, but not for Ru. Although surface core level shifts have never been measured for the (spatially more extented) 3p levels of the second row of transition metals, we believe them to differ not too much from the results for the 3d state, because even the differences for 1s compared with 3d are below 0.1 eV /40/. We obviously need a different explanation. Future theoretical investigations are necessary to clarify the origin of this large blue-shift between substrate photoabsorption and N^+-PSD, in particular of a possible influence of the coupling parameters on the line profiles. For ion PSD from CO/Ru(001) a similar enhancement does not exist at the Ru3p thresholds because PSD-efficient multi-electron states are absent for CO in this energy range.

Conclusions

In summary, we have shown that PSD of neutrals and of ions by core electron excitations are very useful supplementary tools for the investigation of DIET from chemisorbates on metals. Neutrals are the majority species which are of practical importance in technical applications like electron microscopy or any kind of electron beam-based technique, e.g. in semiconductor processing, and ions are ideal probes for highly excited electronic states. Monitored in combination, plentiful information on electronic and nuclear dynamics is obtained. Mass spectrometric detectors are now sensitive enough for studies under high photon energy resolution conditions, at least for systems with not too low cross section. It will be a challenging goal for the future to further improve their performance in order to be able to detect electrons and desorbing neutral particle in coincidence. Such an experiment would yield maximum information on DIET from adsorbates on metal surfaces.

Acknowledgments

We thank the staffs of HASYLAB and BESSY for help during the experiments, in particular T. Möller, C. Nowak, A. Kolmakov, C. Hellwig and C. Jung. We very much thank Norbert Heckmair, who passed away so untimely. Stimulating discussions with W. Wurth are gratefully acknowledged. This study was supported by the Deutsche Forschungsgemeinschaft (projects SFB 338 C10 and Me 266-21/2). S. Frigo acknowledges support by the US Department of Energy, Basic Energy Sciences, Office of Energy under Contract No. W-31-109-ENG-38.

References

1. P. Feulner and D. Menzel, in: *Laser spectroscopy and photochemistry on metal surfaces*, eds: Dai, H. L. and Ho, W. (Singapore, 1995) 627.
2. K. Mase, M. Nagasono, and S. Tanaka, J. Electron. Spectroscopy Rel. Phen 101-103 (1999) 13.
3. K. Mase, M. Nagasono, S. Tanaka, M. Kamada, T. Uriso, and Y. Murata, Rev. Sci. Instrum. 68 (1997) 1703.
4. see, e.g., Z. W. Gortel, R. Teshima, and D. Menzel, Phys. Rev. A (in press).
5. P. Morin and I. Nenner, Phys. Rev. Lett. 56 (1986) 1913.
6. A. Menzel, B. Langer, J. Viefhaus S. B. Whitfield, and U. Becker, Chem. Phys. Lett. 258 (1996) 265.
7. H. Aksela, S. Aksela, J. Tulkki, T. Åberg, G. M. Bancroft, and K.H. Tan, Phys. Rev. A39 (1989) 3401.
8. M. Neeb, A. Kivimäki, B. Kempgens, H. M. Köppe, J. Feldhaus, and A. M. Bradshaw, Phys. Rev. Lett. 76 (1996) 2250.
9. P. Kuiper and B. Dunlap, J. Chem. Phys. 100 (1994) 4087.
10. M. L. Knotek and P. J. Feibelman, Phys. Rev. Lett. 40 (1978) 964.
11. see, e.g., A. Kay, E. Arenhol, S. Mun, F.J. Garcia de Abajo, C.S. Fadley, R. Denecke, Z. Hussain, and M.A. Van Hove, Science 281 (1998) 679.
12. see, e.g., H. Zacharias, Int. J. Mod. Phys. B4 (1990) 45.
13. S. Wurm, P. Feulner, and D. Menzel, Phys. Rev. Lett. 74 (1995) 627.
14. S. P. Frigo, P. Feulner, B. Kassühlke, C. Keller, and D. Menzel, Phys. Rev. Lett. 80 (1998) 2813.

15. R. Romberg, S. P. Frigo, A. Ogurtsov, P. Feulner, and D. Menzel (this volume).

16. R. Weimar, R. Romberg, S. Frigo, B. Kassuehlke, and P. Feulner (this volume).

17. P. Feulner, P. Averkamp and B. Kassühlke, Appl. Phys. A 67 (1998) 657.

18. S. P. Frigo et al., to be published

19. R. Romberg et al., to be published

20. P. Bennich, T. Wiell, O. Karis, M. Weinelt, N. Wassdahl, A. Nilsson, M. Nyberg, L.G.M.Pettersson, J. Stöhr and M. Samant, Phys. Rev. B 57 /1998) 9274, and references therein

21. H. Pfnür, P. Feulner and D. Menzel, J. Chem. Phys. 79 (1983) 4613.

22. P. Feulner and D. Menzel, Phys. Rev. B 25 (1982) 4295.

23. R. Treichler, W. Wurth, E. Riedl, P. Feulner, and D. Menzel, Chem. Phys. 153 (1991) 259

24. H. Ågren and R. Arneberg, Physica Scripta 30 (1984) 55.

25. E. Shigemasa, T. Hayaishi, T. Sasaki, and A. Yagishita, Phys. Rev. A 47 (1993) 1824.

26. R. Arneberg, H. Ågren, J. Müller, and R. Manne, Chem. Phys. Lett. 91 (1982) 362.

27. C. T. Chen, Y. Ma, and F. Sette, Phys. Rev. A 40 (1989) 6373.

28. E. Shigemasa, K. Ueda, Y. Sato, T. Sasaki, and Yagishita, Phys. Rev. A 45 (1992) 2915.

29. K. Lee, D. Y. Kim, C.-I. Ma, and D. M. Hanson, J. Chem. Phys. 100 (1994) 8550.

30. C. Keller, Ph-D. thesis, Technische Universität München 1998.

31. A. Föhlisch, J. Hasselström, O. Karis, P. Väterlein, N. Mårtensson, A. Nilsson, C. Heske, M. Stichler, C. Keller, W. Wurth, and D. Menzel (Chem. Phys. Lett., submitted).

32. D. Menzel and R. Gomer, J. Chem. Phys. 40 (1964) 1164; 41 (1964) 3311; P. A. Redhead, Can J. Phys. 42 (1964) 886.

33. A. Sandell, O. Björneholm, A. Nilsson, E. O. F. Zdansky, H. Tillborg, J. N. Andersen, and N. Mårtensson, Phys. Rev. Lett 70 (1993) 2000.

34. P. Feulner, S. Kulkarni, E. Umbach, and D. Menzel, Surface Sci. 99 (1980) 489.

35. J. A. Misewich, T. F. Heinz and D. M. Newns, Phys. Rev. Lett 68 (1992) 3737.

36. see, e.g., D. L. Dexter, Phys. Rev. 126 (1962) 1962.

37. P. Feulner, R. Treichler, and D. Menzel, Phys. Rev. B 24 (1981) 7427.

38. M. Stichler, Ph-D. thesis, Technische Universität München 1998

39. J. N. Andersen, M. Qvarford, R. Nyholm, S. L. Sorensen, and C. Wigren, Phys. Rev. Lett. 67 (1991) 2822; G. Comelli, M. Sastry, G. Paolucci, K. C. Prince, and L. Olivi, Phys. Rev. B 43 (1991) 14385.

40. J. N. Andersen, D. Hennig, E. Lundgren, M. Methfessel, R. Nyholm and M. Scheffler, Phys. Rev. B 50 (1994) 17525.

Figure captions

Fig.1: PSD of ionic species from CO/Cu(111) and CO/Ru(001), compared with the partial electron yield (PY, from CO/Ru(001)) for O1s excitation. Photon energies are referenced vs. the π-resonance (add 532.6 eV for absolute values).

Fig.2: PY and PSD of neutral species from CO/Cu(111) and CO/Ru(001) for O1s excitation. Photon energies are referenced vs. the π-resonance (add 532.6 eV for absolute values).

Fig.3: PY and PSD of neutral species from N_2/Ru(001) for N1s excitation. For PSD of neutral particles, the pre-threshold signal levels are indicated by short horizontal lines. Photon energies are referenced vs. the π-resonance (add 399.5 eV for absolute values).

Fig.4: PSD of singly and doubly charged N-ions from N_2/Ru(001) by N1s-excitation.

Fig.5: PY and PSD of N^+, N^0 and N_2^0 from N_2/Ru(001) obtained under high photon energy resolution conditions. Varying contributions from N1s excitations of the outer (maximum at 399.1 eV) and the inner (399.8 eV) N atom are obtained for the different signals. PY and PSD signals are displayed as scatter symbols, and the results of the fits based on the analysis of PY data from ref.34 are shown as straight lines.

Fig.6: PY, N^+ and N^{2+} signals from N_2/Ru(001) for $Ru3p_{3/2}$ excitation. The ion-signals are clearly blue-shifted with respect to the PY. Similar results have been obtained for the $Ru3p_{1/2}$ region (not shown).

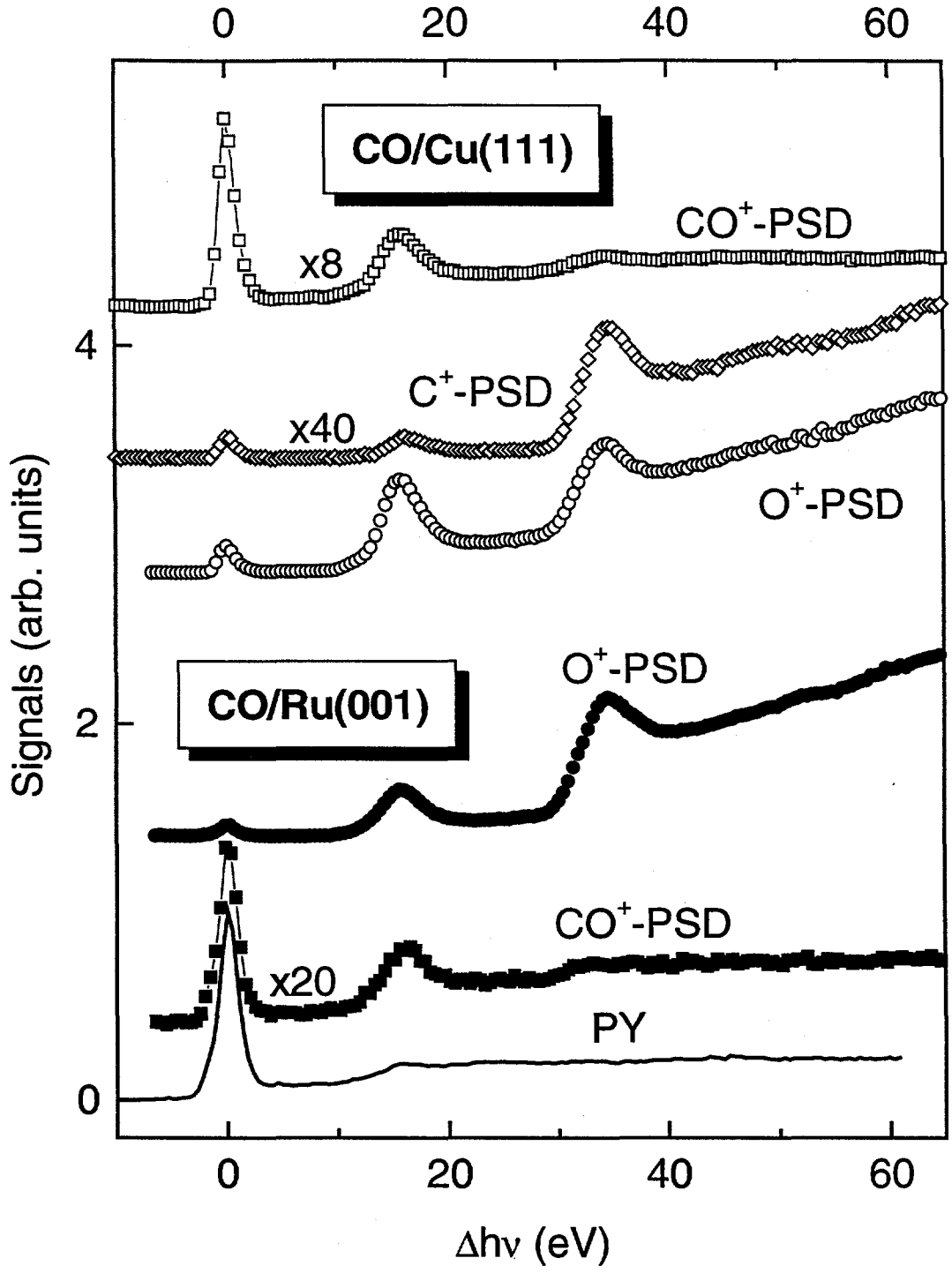
0
20
40
60
CO/Cu(111)
CO+-PSD
x8
C+-PSD
x40
O+-PSD
CO/Ru(001)
O+-PSD
CO+-PSD
x20
PY
4
2
0
Signals (arb. units)
0
20
40
60
Δhν (eV)

Fig.1

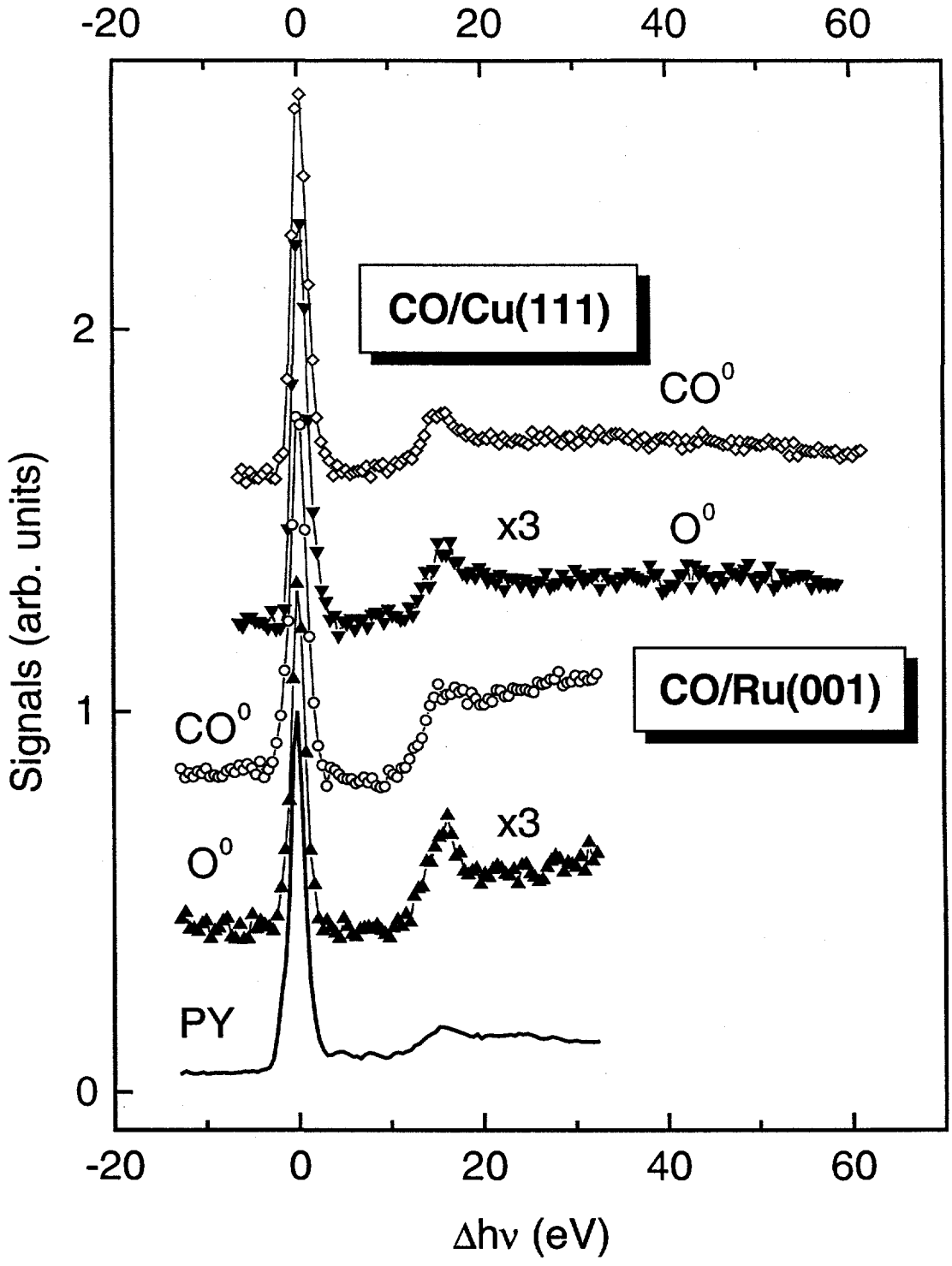
-20
0
20
40
60
CO/Cu(111)
CO⁰
x3
O⁰
CO/Ru(001)
CO⁰
x3
O⁰
PY
2
1
0
Signals (arb. units)
-20
0
20
40
60
Δhν (eV)

Fig.2

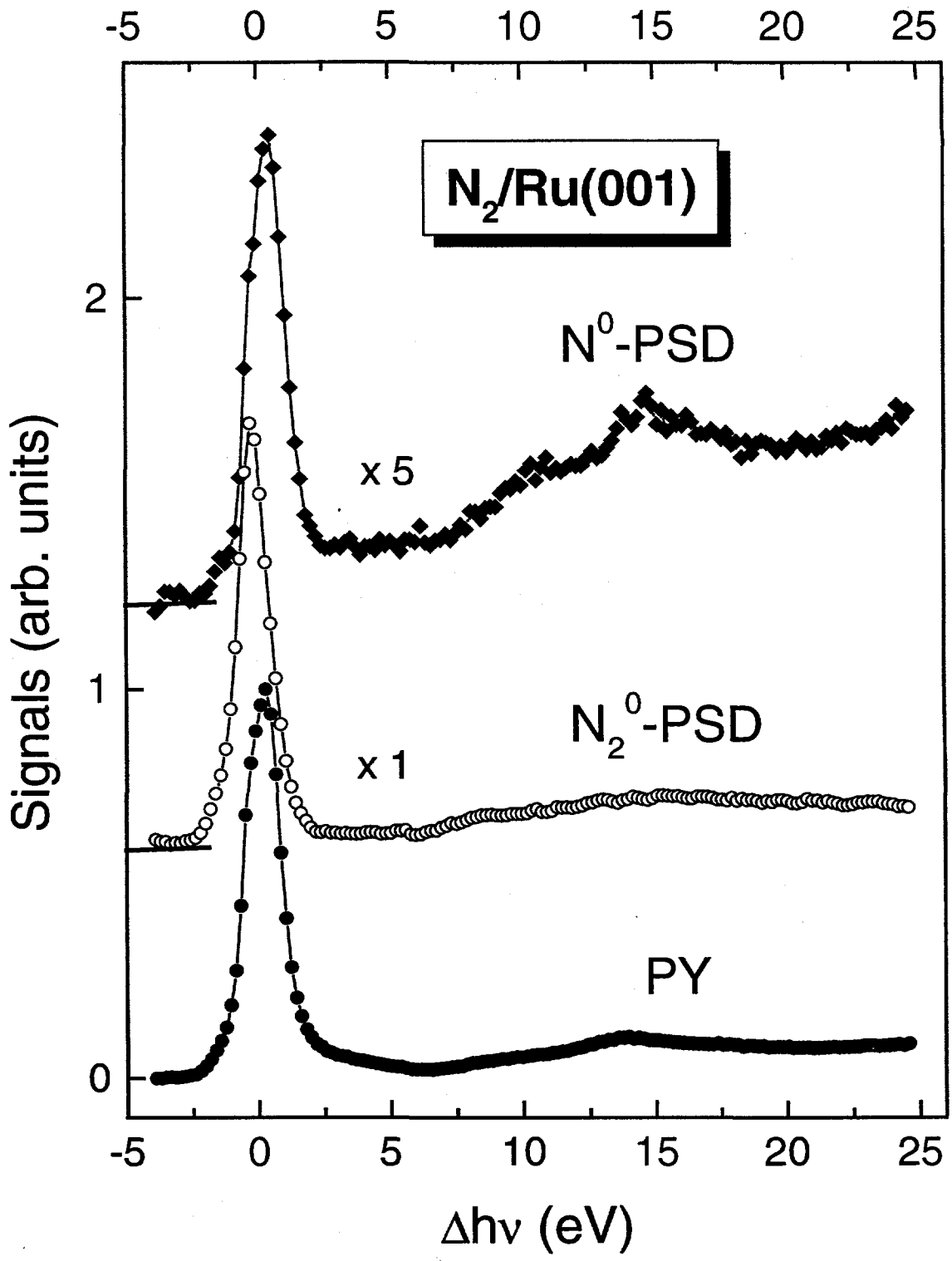
N2/Ru(001)
N0-PSD
x 5
N2 0-PSD
x 1
PY
Signals (arb. units)
Δhν (eV)
-5
0
5
10
15
20
25
0
1
2

Fig.3

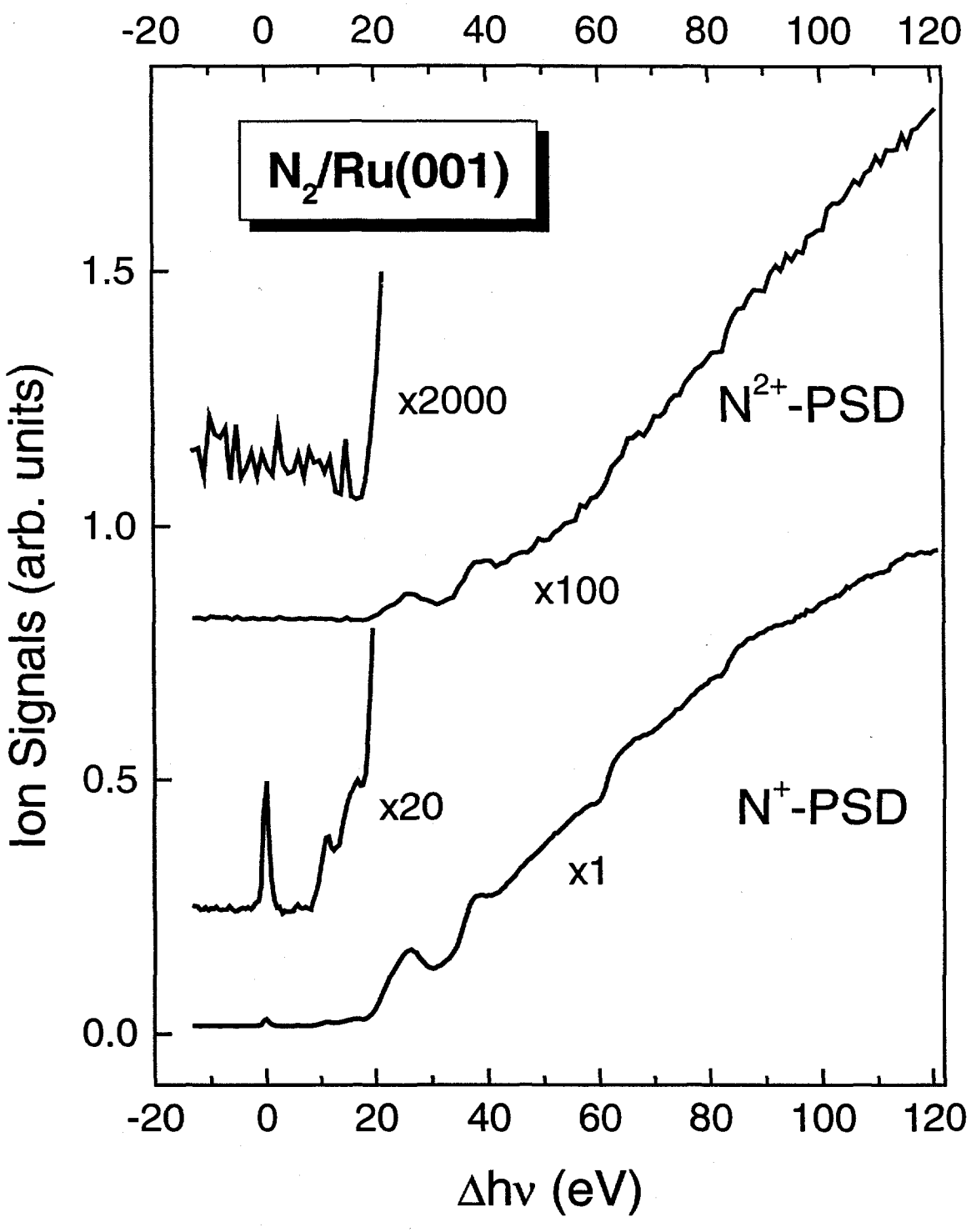
N2/Ru(001)
Ion Signals (arb. units)
Δhν (eV)
N2+-PSD
N+-PSD
x2000
x100
x20
x1
-20
0
20
40
60
80
100
120
0.0
0.5
1.0
1.5

Fig.4

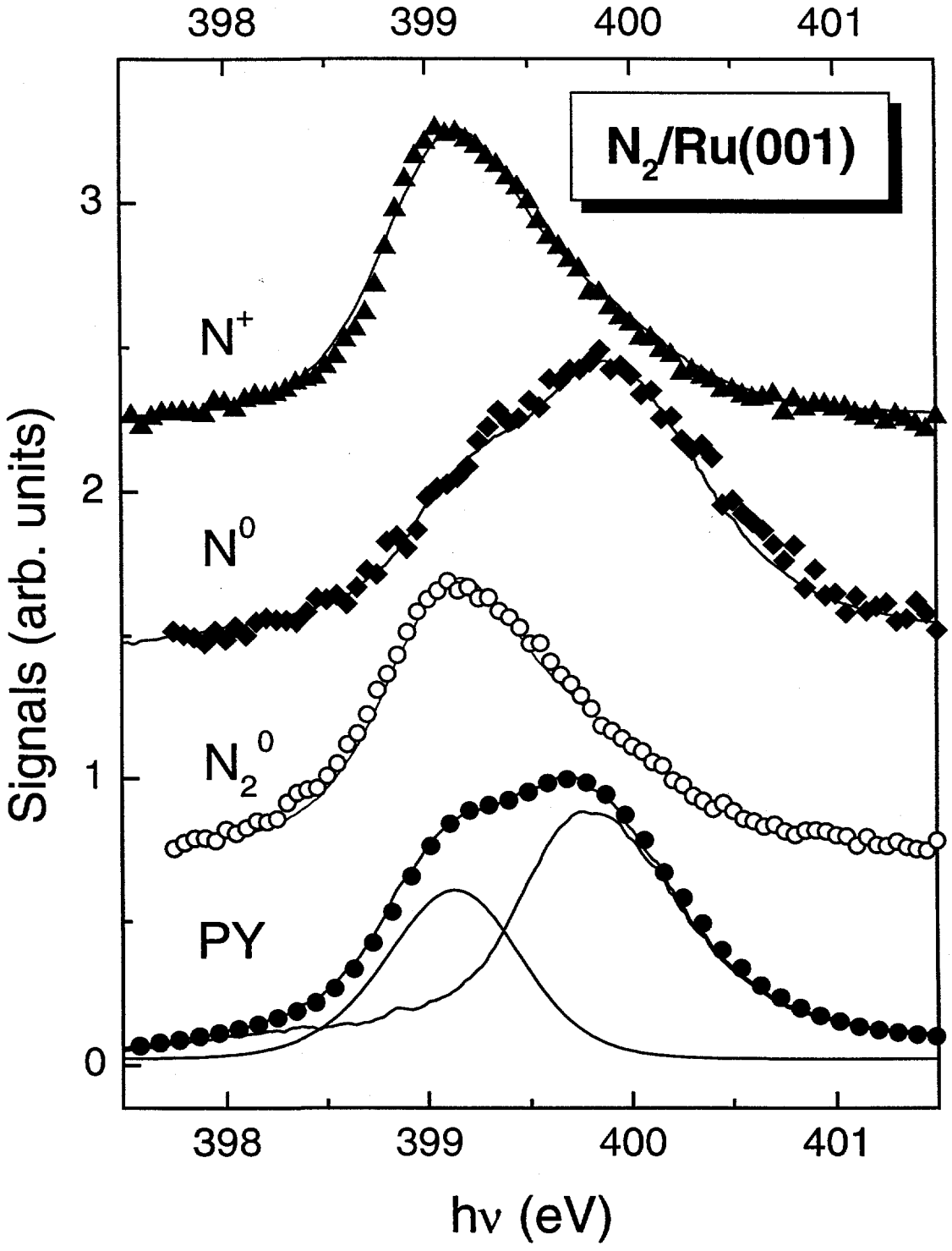
398
399
400
401
N2/Ru(001)
3
2
1
0
N+
N0
N2 0
PY
Signals (arb. units)
398
399
400
401
hν (eV)

Fig.5

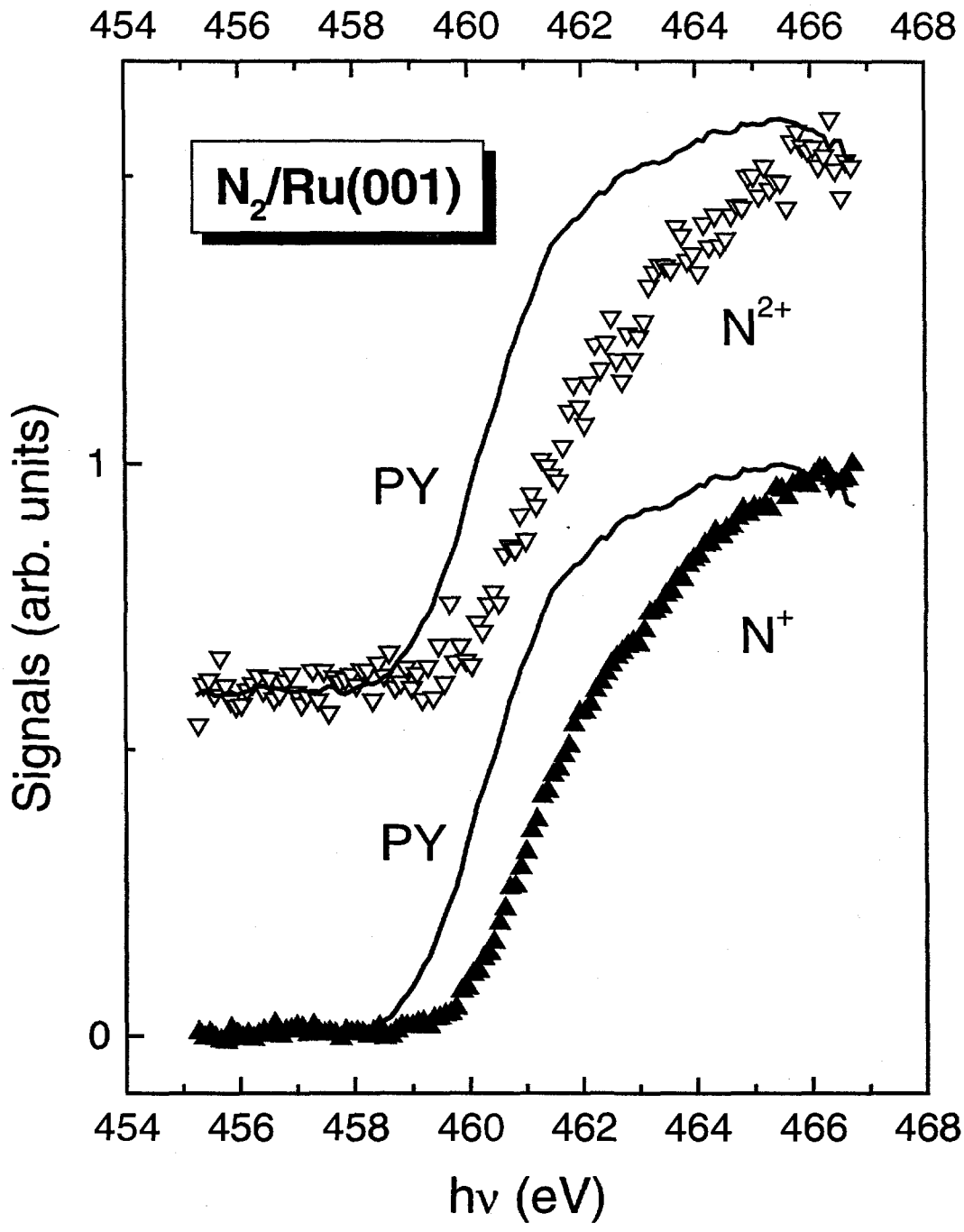
454
456
458
460
462
464
466
468
N2/Ru(001)
N2+
PY
N+
PY
Signals (arb. units)
1
0
454
456
458
460
462
464
466
468
hν (eV)

Fig. 6